Conformational Stability of (+)-Epichlorohydrin

Feng Wang and Prasad L. Polavarapu*

Department of Chemistry, Vanderbilt University, Nashville, Tennessee 37235

Received: February 29, 2000

Vibrational absorption and circular dichroism spectra of (+)-epichlorohydrin have been recorded for the neat liquid and in organic solvents CCl_4, CS_2, $CHCl_3$, CH_2Cl_2, and CH_3I. These spectra are compared with the ab initio predictions of absorption and vibrational circular dichroism (VCD) spectra obtained with density functional theory using the B3LYP/6-311G(2d,2p) basis set for three different conformers of (*S*)-epichlorohydrin. The Boltzmann populations, obtained from Gibbs free energies, indicate that the populations of gauche-II, gauche-I, and cis conformers for isolated molecule are 65, 32, and 3%, respectively. The analysis of experimental and theoretical absorption data indicates that the population ratios of conformers gauche-II:gauche I:cis are: ∼35.7%:∼54.6%:9.7% (neat liquid); ∼58.6%:∼34.0%:7.4% (CCl_4); ∼51.0%:∼40.6%:8.4% (CS_2); ∼46.1%: ∼44.8%:9.1% ($CHCl_3$); ∼42.2%:∼48.5%:9.3% (CH_3I); ∼37.2%:∼53.3%:9.5% (CH_2Cl_2). These compositions are consistent with the experimental VCD spectra. This information clearly indicates that as the polarity of the solvent (as measured by its dipole moment) is increased, the percent composition of the gauche I form increases and that of the gauche II form decreases, but that of cis form is nearly the same in all cases. Vibrational assignments are suggested for the observed bands in the 1500−400-cm^{-1} region, with the fundamentals assigned mainly to the gauche-II and gauche-I conformers.

Introduction

Epichlorohydrin, which is used in the synthesis of the optical isomers of antihypertensive and antianginal agents and in preparation of glycidyl ethers,[1] has been studied using infrared (IR),[2] Raman,[2] nuclear magnetic resonance (NMR),[3] microwave,[4] electron diffraction,[5] and dipole moment[6] measurements. Three different conformations (See Figure 1) have been considered for epichlorohydrin. Based on microwave studies, Fugiwara et al.[4] and Mohammadi et al.[4] concluded that all three conformers, namely, gauche-I, gauche-II, and cis conformers of epichlorohydrin, are present in the vapor phase but their relative populations could not be determined. An electron diffraction study at 67 °C by Shen[5] indicated that the gauche-II form is the most stable (67%) conformer and the gauche-I form is the second most stable (33%) conformer. A small amount of cis form could not be ruled out. Based on electric dipole moments and Kerr constants in cyclohexane solutions, Aroney et al.[6] concluded that the gauche-II form is abundant, with the population of the gauche-II form at 54% and that of the sum of gauche-I and cis forms at 46%. Based on the NMR and dipole moment studies on epichlorohydrin in benzene solutions, Macdonald and Reynolds concluded[3b] that three conformers are present, with the population of the gauche-I form being dominant. Shapiro[3c] reached a similar conclusion that gauche-I is the major conformation and that the combined minimum composition of gauche-II and cis forms is 20% in cyclohexane solution. Solvent was considered to play only a minor role on the conformer population.

Based on vibrational spectroscopic studies, Hayashi et al.[2a] and Charles et al.[2b] suggested that epichlorohydrin exhibits conformational isomerism in the vapor and liquid phases, but only one conformer, gauche-I, is present in the solid state. Both gauche-I and gauche-II forms were suggested to be present in the liquid and vapor phases, with gauche-II being dominant in the vapor phase and gauche-I being dominant in the liquid phase.

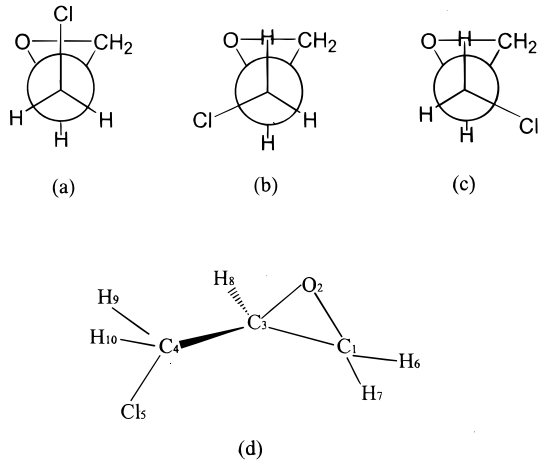

Figure 1. Structures of various forms of (*S*)−(+)-epichlorohydrin: (a) cis-Cl conformation, (b) gauche-I conformation; (c) gauche-II conformation; and (d) absolute configuration.

The presence of a small amount of cis form could not be ruled out. This result suggested a change in the relative populations from vapor to liquid phase. However, differences in populations between neat liquid and solution phases were not addressed in these two studies. In another vibrational spectroscopic study, Kalasinsky et al.[2c] concluded that the gauche-I form is more stable in both the liquid and vapor phases. More recently, based on IR and Raman studies, Lee et al.[2d] concluded that the gauche-II conformer is the most stable form and the gauche-I conformer is the second most stable form in xenon solution, whereas the gauche-I conformer is the most stable form and the cis conformer is the second most stable form in neat liquid.

Based on the review of the literature just given, three questions pertaining to the conformations of epichlorohydrin remain. (a) Except for the studies of Kalasinsky et al.,[2c] there is a general agreement that epichlorohydrin in the vapor phase

10.1021/jp000757c CCC: $19.00
Published on Web 06/03/2000

exists in all three conformations with the gauche-II conformer being more abundant. The relative populations of these conformers in the vapor phase derived from electron diffraction data[5] remain to be verified at least by one other method. (b) In liquid solutions, some studies indicated the gauche-I conformer to be dominant whereas others indicated the gauche II conformer to be dominant. For neat liquid, the gauche I conformer is considered to be dominant, but some studies suggested the gauche-II conformer as the second most stable, whereas the latest study[2d] concluded the cis conformer to be the second most stable. Thus, there are disagreements on the composition of conformers of epichlorohydrin in liquid solutions and in neat liquid. (c) In xenon solutions, the major conformer is found to be same as that in vapor phase, but it is not clear if this observation applies to inert organic solvents as well. Thus, the population differences among the neat liquid and solution phases remains to be established.

Recent studies have shown that the experimental measurements of IR absorption and vibrational circular dichroism (VCD) along with ab initio calculations can provide a powerful approach for determining conformational behavior of chiral molecules.[7] VCD studies on epichlorohydrin have not been reported before.

In the present work, vibrational absorption and vibrational circular dichroism spectra were measured, and theoretical ab initio calculations were performed with the Gaussian 98 program[8] to investigate the relative stability and the energy differences among the three conformations of epichlorohydrin. The ab initio calculations using density functional theory (DFT)[9] and the B3LYP/6-311G(2d,2p) basis set[8] were carried out to obtain the optimized structures and energies. The same level of theory has also been used to predict the vibrational absorption and VCD spectra of different conformers. Based on the comparison of the experimental absorption and VCD spectra with the corresponding ab initio predictions, the compositions of conformations of (+)-epichlorohydrin in neat liquid and in different organic solvents have been suggested.

Procedures

The sample of (+)-epichlorohydrin was obtained from Aldrich Chemical Company at a stated purity of 99%. The IR absorption and VCD spectra in the 2000−900-cm^{-1} region were recorded on a commercial Fourier transform VCD spectrometer, Chiralir (Bomen-Bio Tools, Canada). The VCD spectra were recorded with a 1-h data collection time at 4 cm^{-1} resolution. The absorption spectra in 4000−400-cm^{-1} region were also measured with a Genesis (ATI Mattson) Fourier-transform infrared (FTIR) spectrometer. Spectra were measured for the neat liquid (path length is 14 μm) and in CCl_4 (0.495 M), CS_2 (0.480 M), $CHCl_3$ (0.593 M), CH_2Cl_2 (0.534 M), and CH_3I (0.673 M) solvents. The sample was held in a variable or fixed path length cells with BaF_2 or KBr windows. In the presented absorption spectra (see Figure 2), the solvent absorption was subtracted out. In the presented VCD spectra (see Figure 3), the raw VCD spectrum of the solvent was subtracted. The spectra only show the regions where interference of solvents is minimal.

The ab initio vibrational frequencies, absorption, and VCD intensities for (*S*)-epichlorohydrin were calculated using the Gaussian 98 program[8] on a Pentium II 300 MHz PC. The predictions obtained with DFT with the B3LYP functional[9] and 6-31G* basis set were not in satisfactory agreement with the experimental data. Thus, the calculations were done with the B3LYP functional and larger 6-311G(2d, 2p) basis set. The

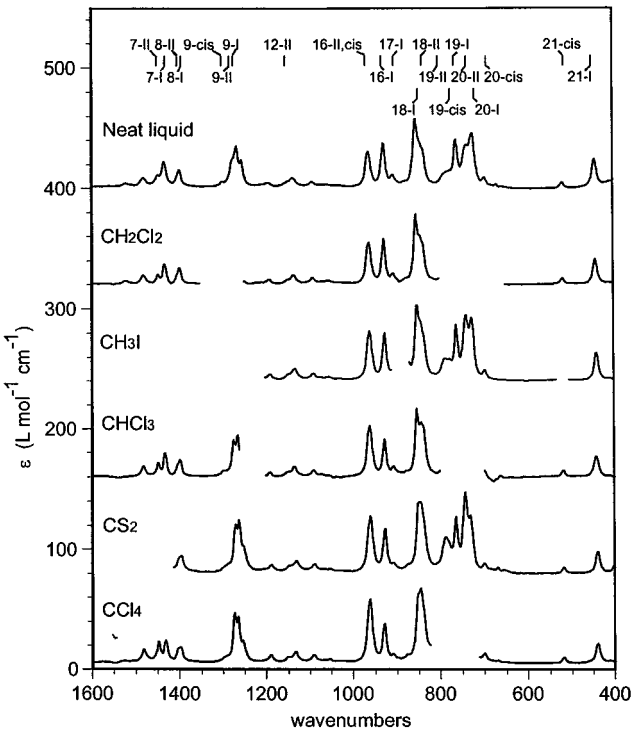

Figure 2. Experimental absorption spectra of (+)-epichlorohydrin in different solvents in the 1600−400-cm^{-1} region. The labels on the traces indicate the solvent used. The labels for the peaks are same as those in Table 6.

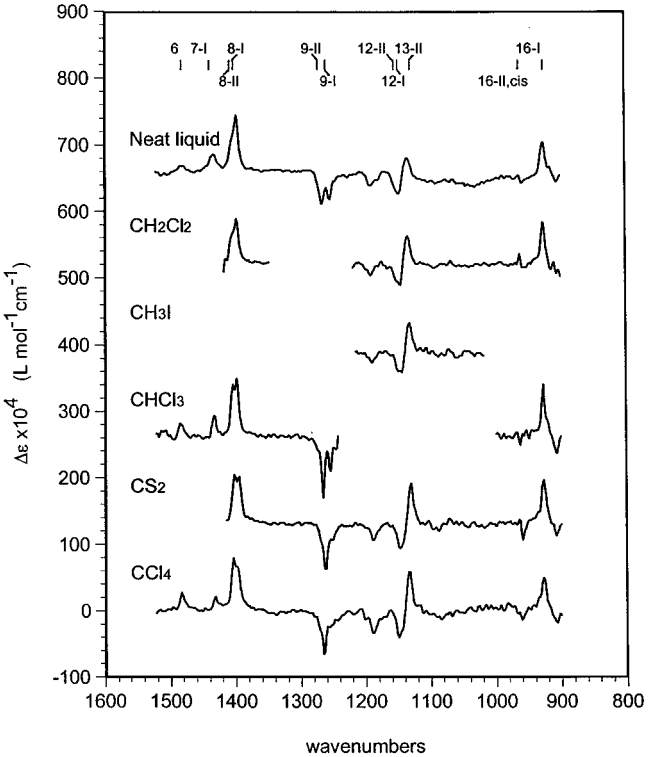

Figure 3. Experimental VCD spectra of (+)-epichlorohydrin in different solvents in the 1600−900-cm^{-1} region. The labels on the traces indicate the solvent used. The labels for the peaks are same as those in Table 6.

procedure for calculating the VCD intensities using DFT theory is that of Cheeseman et al.[10] as implemented in the Gaussian 98 program.[8] The theoretical absorption and VCD spectra were simulated with Lorentzian band shapes and 8 cm^{-1} full width at half-height (fwhh). Because the ab initio predicted band

TABLE 1: Conformations and Energies of (*S*)-Epichlorohydrin

type	starting geom. Cl−C−C*−C[a]	converged geom. Cl−C−C*−C[a]	energy[b] Electronic	energy[b] Gibbs	ΔE[c] (kcal/mol)	Pop.[d] (%)
cis	0	20.9	−652.790163	−652.742400	1.794	3.1
gauche I	120	151.9	−652.792214	−652.744575	0.429	31.6
gauche II	−120	−92.9	−652.792858	−652.745259	0.0	65.3

[a] Dihedral angle. [b] In Hartrees. [c] Relative energy difference. [d] Percent population based on Gibbs energies.

TABLE 2: Structural Parameters of (*S*)-Epichlorohydrin

	B3LYP/6-311G(2d,2p)			MP2/6-31G*[b]			Microwave[b]		
parameter[a]	g-II	g-I	cis	g-II	g-I	cis	g-II	g-I	cis
$R(C_3-C_4)$	1.500	1.495	1.505	1.501	1.497	1.507	1.522	1.513	1.522
$R(Cl-C_4)$	1.820	1.821	1.810	1.787	1.787	1.779	1.767	1.760	1.794
$R(C_1-C_3)$	1.463	1.469	1.463	1.463	1.467	1.463	1.471	1.471	1.471
$R(C_3-O)$	1.431	1.426	1.421	1.439	1.435	1.431	1.436	1.436	1.436
$R(C_1-O)$	1.436	1.430	1.437	1.445	1.442	1.447	1.436	1.436	1.436
$R(H_8-C_3)$	1.085	1.085	1.089	1.090	1.090	1.093	1.082	1.082	1.082
$R(H_9-C_4)$	1.086	1.087	1.087	1.091	1.091	1.093	1.092	1.092	1.092
$R(H_{10}-C_4)$	1.085	1.086	1.087	1.091	1.092	1.092	1.092	1.092	1.092
$R(H_6-C_1)$	1.084	1.084	1.084	1.087	1.088	1.088	1.082	1.082	1.082
$R(H_7-C_1)$	1.084	1.085	1.082	1.088	1.088	1.086	1.082	1.082	1.082
$A(C_4-C_3-H_8)$	115.7	115.6	111.4	115.8	115.7	112.0			
$A(C1-C_4-C_3)$	110.4	111.5	114.5	110.1	111.0	113.8	111.0	109.5	110.9
$A(C_4-C_3-C_1)$	121.0	120.2	125.4	46.5	46.2	51.9			
$A(O-C_3-C_4)$	114.3	116.7	118.4	154.8	144.8	151.6			
$A(C_1-O-C_3)$	61.4	61.9	61.6	67.7	76.8	75.6			
$A(H_9-C_4-C_3)$	111.1	111.4	110.3	111.3	109.8	109.5	109.5	109.5	109.5
$A(H_{10}-C_4-C_3)$	111.8	111.0	110.2	110.0	111.0	109.6	109.5	109.5	109.5
$A(H_6-C_1-C_3)$	119.4	119.2	119.1	119.1	119.7	119.6			
$A(H_7-C_1-C_3)$	119.3	119.6	119.4	119.8	119.5	119.3			
$A(H_6-C_1-H_7)$	115.9	115.7	116.4	115.7	115.6	116.2			
$D(Cl-C_4-C_3-H_8)$	62.5	−55.4	173.9	62.6	−57.3	−182.5	70.2	−54.0	−173.2

[a] Bond lengths in Å; bond angles in degrees; energy in Hartrees. [b] Dihedral angles from MP2/6-31G* data (ref 2d) and microwave data (refs 4a and 4c) given for (*R*)-epichlorohydrin were multiplied by −1.

positions are higher than the experimental values, the ab initio frequencies were scaled with 0.975.

For the normal coordinate analysis, the following procedure was used to transform the ab initio results into the form required for our normal coordinate analysis programs. The Cartesian coordinates obtained for the optimized structure were input into the G-matrix program[11] together with the definitions of 24 internal coordinates. The B-matrix obtained in the output was then converted to local internal symmetry coordinates which was then used to convert the ab initio force field in Cartesian coordinates to a force field in the local internal symmetry coordinates. The force constants were then input, along with the symmetrized B-matrix, into the vibrational optical activity program developed in our laboratory to calculate the potential energy distribution (PED) for all three conformers.

Results and Discussion

Three possible conformations of (*S*)-epichlorohydrin, differing in the dihedral angle Cl−C−C*−C (Figure 1) and labeled as gauche-II, gauche-I, and cis, were investigated. Using the starting Cl−C−C*−C dihedral angles of −120° for gauche-II, +120° for gauche-I, and 0° for cis, the geometries were optimized with the B3LYP/6-311G(2d, 2p) basis set. The converged Cl−C−C*−C dihedral angles, optimized energies, and relative populations based on the Gibbs free energies are listed in Table 1. Based on the ab initio predicted Gibbs energies, it can be concluded that the isolated (*S*)-epichlorohydrin molecule exists predominantly in two conformations, gauche-II (65.3%) and gauche-I (31.6%). These relative populations, which are expected to be applicable for epichlorohydrin in the vapor phase, are close to the populations derived from the electron diffraction data[5] as 67% for gauche-II and 33% for gauche-I.

The structural parameters for all three conformers are listed in Table 2 and compared with those obtained from MP2/6-31G* calculations[2d] and those derived[4c,4d] from microwave spectra. There are some significant differences among the structural parameters (for example, the C_1-O-C_3 and $O-C_3-C_4$ angles) obtained in the present DFT and literature MP2/631G* calculations. Because the vibrational spectra predicted with the 6-311G-(2d, 2p) basis set are in good agreement with the experimental spectra (vide infra), but those predicted with the 6-31G* basis set are not, the structural parameters obtained in the present B3LYP/6-311G(2d, 2p) calculations are believed to be more accurate.

All three conformers investigated were found to have energy minima (all vibrational frequencies are real at the B3LYP/6-311G(2d, 2p) level), so the absorption and VCD intensities were calculated for all of them at the B3LYP/6-311G(2d,2p) level. The internal coordinates and local symmetry coordinates needed for calculating the potential energy distribution are given in Tables 3 and 4. The PED values for all vibrations of three conformers are given in Table 5. Table 6 summarizes the predicted and experimental frequencies and vibrational assignments based on PED. In Table 6 the calculated frequencies are obtained from the peak absorption positions in the simulated population weighted theoretical spectra, whereas predicted frequencies are obtained by scaling the calculated frequencies with 0.975. The predicted frequencies match the observed frequencies reasonably well. The band numbers in Table 6 and in figures are appended with conformation labels; for example,

TABLE 3: Internal Coordinate[a] Definitions for (*S*)-Epichlorohydrin

no.	coordinate	no.	coordinate	no.	coordinate
R_1	C_1O_2 stretch	R_{11}	$O_2C_1H_6$ bend	R_{21}	$C_3C_4Cl_5$ bend
R_2	C_1C_3 stretch	R_{12}	$O_2C_1H_7$ bend	R_{22}	$C_3C_4H_9$ bend
R_3	C_1H_6 stretch	R_{13}	$O_3C_1H_6$ bend	R_{23}	$C_3C_4H_{10}$ bend
R_4	C_1H_7 stretch	R_{14}	$C_3C_1H_7$ bend	R_{24}	$Cl_5C_4H_9$ bend
R_5	O_2C_3 stretch	R_{15}	$H_6C_1H_7$ bend	R_{25}	$Cl_5C_4H_{10}$ bend
R_6	C_3C_4 stretch	R_{16}	$C_1C_3C_4$ bend	R_{26}	$H_9C_4H_{10}$ bend
R_7	C_3H_8 stretch	R_{17}	$C_1C_3H_8$ bend	R_{27}	$C_1O_2C_3$ bend
R_8	C_4Cl_5 stretch	R_{18}	$O_2C_3C_4$ bend	R_{28}	$C_1C_3O_2$ bend
R_9	C_4H_9 stretch	R_{19}	$O_2C_3H_8$ bend	R_{29}	$O_2C_1C_3$ bend
R_{10}	C_4H_{10} stretch	R_{20}	$C_4C_3H_8$ bend	R_{30}	$H_8C_3C_4Cl_5$ torsion

[a] For atom labels see Figure 1.

TABLE 4: Local Symmetry Coordinates[a] for (*S*)-Epichlorohydrin

no.	definition	discription
S_1	R_3-R_4	$H_6C_1H_7$ antisymmetric stretch
S_2	R_9-R_{10}	$H_9C_4H_{10}$ antisymmetric stretch
S_3	R_7	C_3-H_8 stretch
S_4	R_3+R_4	$H_6C_1H_7$ symmetric stretch
S_5	R_9+R_{10}	$H_9C_4H_{10}$ symmetric stretch
S_6	$4R_{15}-R_{11}-R_{12}-R_{13}-R_{14}$	$H_6C_1H_7$ deformation
S_7	R_{26}	$H_9C_4H_{10}$ deformation
S_8	$R_5+R_1+R_2$	ring breathing
S_9	$R_{22}+R_{23}-R_{24}-R_{25}$	$H_9C_4H_{10}$ rock
S_{10}	$2R_{20}-R_{19}-R_{17}$	C−H in-plane bend
S_{11}	$R_{22}-R_{23}$	$H_9C_4H_{10}$ wag
S_{12}	$R_{19}-R_{17}$	C−H out-of-plane bend
S_{13}	$R_{11}+R_{12}-R_{13}-R_{14}$	$H_6C_1H_7$ wag
S_{14}	$R_{24}-R_{25}$	$H_9C_4H_{10}$ twist
S_{15}	$R_{11}-R_{12}+R_{13}-R_{14}$	$H_6C_1H_7$ rock
S_{16}	R_6	C_3-C_4 stretch
S_{17}	$R_{11}-R_{12}-R_{13}+R_{14}$	$H_6C_1H_7$ twist
S_{18}	$2R_{27}-R_{28}-R_{29}$	ring symmetric deformation
S_{19}	R_5-R_1	ring antisymmetric deformation
S_{20}	R_8	C−Cl stretch
S_{21}	$R_{16}-R_{18}$	ring-$C(Cl)H_2$ bend
S_{22}	$R_{16}+R_{18}$	ring-$C(Cl)H_2$ bend
S_{23}	R_{21}	CCCl bend
S_{24}	R_{30}	$H_8C_3C_4Cl_5$ torsion

[a] Unnormalized; internal coordinates R_k are defined in Table 3. These definitions of local symmetry coordinates are same as those in ref 2d.

the bands ν_{9-cis}, ν_{9-I}, and ν_{9-II} represent, respectively, the ninth vibrational band of cis, gauche-I, and gauche-II conformers.

The predicted absorption and VCD spectra (with calculated frequencies scaled by 0.975) simulated with 8 cm^{-1} half-widths and Lorentzian band shapes for (*S*)-epichlorohydrin are shown in Figures 4 and 5. The predicted spectra for individual conformers (labeled a, b, and c) as well as for the composition of conformers derived from Gibbs energies (labeled "Pred.") are shown in these figures. A comparison of these spectra with the experimental spectra in Figures 2 and 3 indicates that the spectra predicted for no one conformation match the experimental spectra. Also the spectra predicted for the composition derived from the Gibbs energies do not match well with the experimental spectra. In the experimental absorption spectrum of neat liquid, the intensity at 1431 cm^{-1} is larger than that at 1447 cm^{-1} and the intensity at 930 cm^{-1} is slightly larger than that at 960 cm^{-1}. However, in the experimental absorption spectrum in CCl_4 solution, the intensities at 1431 and 1447 cm^{-1} are nearly the same, and the intensity at 960 cm^{-1} is larger than that at 930 cm^{-1}, which is in contrast to those in the neat liquid. These observations clearly suggest that the relative population of the conformations in neat liquid has changed from that in CCl_4 solution. Thus it can be concluded that more than one conformation is present in the liquid/solution phase, and the composition of conformations here is not same as that predicted for an isolated molecule.

The theoretical spectra can be analyzed to find the bands that are characteristic to each of the three conformers and the intensities of those characteristic bands can be used to determine the composition of conformers. For determining the conformer populations, Lee et al.[2d] used the bands in the 920−970-, 850−830-, 795−760-, and 530−400-cm^{-1} regions. In the 920−970-cm^{-1} region, we note that calculated band (Table 5) ν_{16} for gauche I conformer (at 945 cm^{-1}) is well separated from those for gauche II (978 cm^{-1}) and cis (985 cm^{-1}) conformers. Based on this prediction, the experimental band (Table 6) at 930 cm^{-1} is assigned to gauche-I conformer and that at 960 cm^{-1} is assigned to both gauche II and cis conformers. The same assignments were proposed by Lee et al.[2d] The assignments suggested by Kalasinsky et al.,[2c] that the 930 and 960 cm^{-1} bands belong to the same conformer, are clearly incorrect. The bands in 850−830- and 795−760-cm^{-1} regions are not well resolved in the present liquid-phase spectra at room temperature, so we could not use the intensities in this region unambiguously. The C−Cl stretching bands appearing in the second region at 743, 731, and 699 cm^{-1} were assigned by Kalasinsky et al.[2c] to the cis, gauche-I, and gauche-II conformations, respectively. But Lee et al.[2d] assigned these three bands to gauche-II, gauche-I, and cis conformers, respectively. The present assignments (Table 6) are in agreement with those derived from MP2/6-31G* calculations of Lee et al.[2d] In the 530−400-cm^{-1} region, the calculated band (Table 5) ν_{21} for gauche-I conformer (435 cm^{-1}) is well separated from that for cis conformer (517 cm^{-1}). The corresponding band for gauche II conformer is predicted to have very low absorption intensity. Based on these observations, the experimental absorption band at 439 cm^{-1} is assigned to the gauche-I conformer and that at at 518 cm^{-1} is assigned to cis conformer (Table 6). These assignments are in agreement with those of Lee et al.[2d] In summary, in the 1600−400-cm^{-1} region, the bands at 960 and 930 cm^{-1} and 518 and 439 cm^{-1} represent two pairs of well-separated conformer-dependent absorption bands, for liquid solutions at room temperature, whose intensities provide information about conformer populations.

With these assignments and using calculated absorption intensities (Table 5) for individual conformer bands, one can set up two equations relating conformer populations to the areas of the observed bands at 960 and 930 cm^{-1} and at 518 and 439 cm^{-1}. These equations, along with the constraint that the sum of populations of three conformers is 100%, permit us to calculate the individual conformer populations from the experimental absorption band areas. The same procedure is, in principle, applicable for VCD bands, but the VCD intensity predicted (and also observed) for ν_{16} is very small for gauche II and cis conformers. Furthermore, VCD measurements at the present time are restricted to the region above ~900 cm^{-1}, so VCD intensities for ν_{21} are not measurable. For these reasons, the populations of individual conformers are determined solely from the experimental absorption intensity data and summarized in Table 7. Nevertheless, VCD data can provide a cross check to verify if the predicted VCD with these populations matches the experimentally observed VCD in the 1600−900 cm^{-1} region. For this purpose, theoretical spectra were simulated for four different compositions: (a) composition obtained from Gibbs free energies (these spectra are labeled "Pred."); (b) composition deduced from neat liquid absorption spectra (these spectra are labeled "Cal.1"); (c) composition deduced from absorption spectra in CS_2 solvent (these spectra are labeled "Cal.2"); and (d) composition deduced from absorption spectra in CCl_4 solvent

TABLE 5: Calculated Frequencies, Absorption Intensities and VCD Intensities for (*S*)−(+)-Epichlorohydrin[a]

	gauche II				gauche I				cis			
no.	freq.[a]	*A*	*R*	PED[b]	freq.[a]	*A*	*R*	PED[b]	freq.[a]	*A*	*R*	PED[b]
ν_1	3186	20.23	−2.26	S_1	3178	21.97	−3.44	S_1	3198	12.74	−2.71	S_1
ν_2	3161	5.36	7.10	S_2	3158	4.19	−2.52	S_2	3137	3.78	−4.09	S_2
ν_3	3126	9.34	3.17	S_3	3125	9.11	−0.20	S_3	3103	23.95	7.16	S_4
ν_4	3100	10.19	−5.41	S_5	3093	21.49	8.52	S_5, S_4	3089	32.59	−7.59	S_5, S_3
ν_5	3096	21.02	−2.43	S_4	3090	15.47	−3.44	S_4, S_5	3073	7.47	−3.73	S_3, S_5
ν_6	1532	1.96	6.24	S_6, S_8	1531	2.14	3.77	S_6, S_8	1530	6.19	7.01	S_6, S_8
ν_7	1493	6.38	−0.39	S_7	1471	9.68	6.91	S_7	1475	4.45	−1.45	S_7
ν_8	1440	5.14	13.52	S_{10}, S_8	1431	5.71	17.73	S_{10}, S_8	1432	17.55	2.87	S_{10}, S_8
ν_9	1299	23.28	−9.59	S_9, S_8	1288	31.32	−28.60	S_9, S_{10}	1315	18.34	8.98	S_9, S_{16}
ν_{10}	1271	5.17	3.54	S_9, S_{10}	1280	11.13	1.65	S_8, S_9	1296	5.42	−4.93	S_{10}, S_8
ν_{11}	1209	4.49	−13.28	S_{11}, S_{14}	1228	0.27	1.10	S_{11}, S_{14}	1229	0.97	−4.06	S_{11}, S_{14}
ν_{12}	1174	1.13	−8.52	S_{12}, S_{15}	1165	1.36	−10.39	S_{12}, S_{15}	1169	0.92	−5.29	S_{13}, S_{12}
ν_{13}	1156	0.96	5.57	S_{13}, S_8	1162	1.66	6.73	S_{13}, S_{12}	1157	1.30	4.68	S_{15}, S_{13}
ν_{14}	1112	4.68	−2.93	S_{17}, S_{15}	1108	1.91	1.53	S_{14}, S_{16}	1093	0.64	−1.17	S_{17}, S_{12}
ν_{15}	1068	1.03	−2.19	S_{12}, S_{14}	1093	1.10	1.27	S_{12}, S_{15}	1042	2.13	−3.72	S_{17}, S_{12}
ν_{16}	978	28.85	−1.65	S_{18}, S_{16}	945	25.52	31.00	S_{18}, S_{17}	985	29.55	4.32	S_{18}, S_{14}
ν_{17}	890	3.38	−4.74	S_{17}, S_{11}	925	2.48	−16.95	S_{19}, S_{14}	915	3.34	−12.00	S_{19}, S_{11}
ν_{18}	858	22.88	4.08	S_{19}, S_{18}	861	25.00	−34.33	S_{18}, S_{17}	849	29.29	15.36	S_{18}, S_{11}
ν_{19}	810	14.72	13.26	S_{19}, S_{18}	787	21.94	33.64	S_{19}, S_{16}	791	18.98	17.23	S_{19}, S_{20}
ν_{20}	725	64.18	−0.11	S_{20}, S_{23}	715	42.3	6.12	S_{20}, S_{23}	639	16.52	−23.82	S_{20}, S_{23}
ν_{21}	408	0.16	−0.78	S_{21}, S_{22}	435	14.55	−39.44	S_{21}, S_{22}	517	13.44	9.39	S_{22}, S_{20}
ν_{22}	370	3.81	−7.18	S_{22}, S_{20}	363	2.02	8.86	S_{22}, S_{20}	354	7.86	−4.91	S_{21}
ν_{23}	209	11.16	−11.94	S_{23}, S_{21}	209	0.17	3.99	S_{23}, S_{21}	202	0.59	−1.70	S_{23}, S_{22}
ν_{24}	89	6.70	19.56	S_{24}, S_{21}	96	1.16	6.04	S_{24}, S_{21}	106	3.41	−0.42	S_{24}, S_{23}

[a] Frequencies in cm^{-1}, absorption intensities (*A*) in Km/mol; and rotational strengths (*R*) in 10^{-44} esu^2cm^2, obtained with B3LYP/6-311G(2d,2p) basis set. [b] Local symmetry coordinates with largest contributions to potential energy distribution (PED); for symmetry coordinate definitions, see Table 4.

TABLE 6: Comparison of Predicted and Observed Wavenumbers for (*S*)-Epichlorohydrin

band no.[a]	exp. (cm^{-1})[b]	pred. (cm^{-1})[c,d]	calc. (cm^{-1})[c,e]	assignment[f]
ν_6	1481	1493	1531	*CH_2 deformation
ν_{7-II}	*1447	1456	1493	CH_2 deformation
ν_{7-I}	1431	1434	1471	CH_2 deformation
ν_8	1400	1404	1440	C−H in-plane bend, ring breathing
ν_{9-cis}	*1300	1282	1315	CH_2 rock, ring breathing
ν_{9-II}	1273	1267	1299	CH_2 rock, ring breathing
ν_{9-I}	1253	1256	1288	CH_2 rock, ring breathing
ν_{10}		1248	1280	ring breathing
ν_{11-II}	1188	1179	1209	CH_2 wag
ν_{12-II}	*1156	1145	1174	C−H out-of-plane bend
ν_{13}	1134	1127	1156	*CH_2 wag, HCH bend
ν_{14}	1092	1084	1112	*CH_2 twist
ν_{15}	1053	1041	1068	C−H out-of-plane bend, CH_2 twist
$\nu_{16-II,cis}$	960	954	978	ring symmetric deformation, CC stretch
ν_{16-I}	930	921	945	ring symmetric deformation, CC stretch
ν_{17-I}	906	902	925	ring antisymmetric deformation
ν_{17-II}	*872	868	890	*CH_2 twist
ν_{18}	853	837	858	ring deformation
$\nu_{19-II, cis}$	*787	781	801	ring antisymmetric deformation
ν_{19-I}	764	767	787	ring antisymmetric deformation
ν_{20-II}	*743	706	725	C−Cl stretch
ν_{20-I}	731	697	715	C−Cl stretch
ν_{20-cis}	699	623	639	C−Cl stretch
ν_{21-cis}	518	504	517	ring-C(Cl)H_2 bend
ν_{21-I}	439	424	435	ring-C(Cl)H_2 bend

[a] These numbers derived from those in Table 5, and the subscripts I, II, or cis indicate the conformation contributing to the intensity of the band. [b] Experimental wavenumbers obtained from the absorption spectrum at concentration of 0.495 M (CCl_4); asterisks (*) denote those bands that appear as shoulders in the spectrum collected for the neat liquid. [c] Band positions from the spectra simulated with populations given in Table 1. [d] Ab initio wavenumbers scaled with 0.975. [e] Unscaled ab initio wavenumbers. [f] See Table 5 for vibrational assignments; asterisks (*) denote ring modes.

(these spectra are labeled "Cal.3"). These predicted spectra are compared with the experimental spectra in Figures 6−7.

In the experimental absorption spectrum of neat liquid, the intensity of ν_{7-I} is greater than that of ν_{7-II} and the intensity of ν_{16-I} is greater than that of $\nu_{16-II,cis}$. These features are correctly reproduced in the Cal.1 spectrum (see Figure 6). In the experimental absorption spectrum obtained in CCl_4 solution, the intensities of ν_{7-I} and ν_{7-II} are nearly equal and the intensity of ν_{16-I} is less than that of $\nu_{16-II,cis}$. These features are correctly reproduced in the Cal.3 spectrum. In CS_2 solution, the ν_{7-I} and ν_{7-II} bands could not be measured because of solvent absorption interference, but ν_{16-I} and ν_{16-II} have the same pattern as that in CCl_4 solution, which is reproduced in Cal.2 spectrum. In all three cases, absorption bands in the 1200−1300-cm^{-1} region are better resolved in the experimental spectra than in predicted spectra. In the experimental VCD spectrum of neat liquid, the

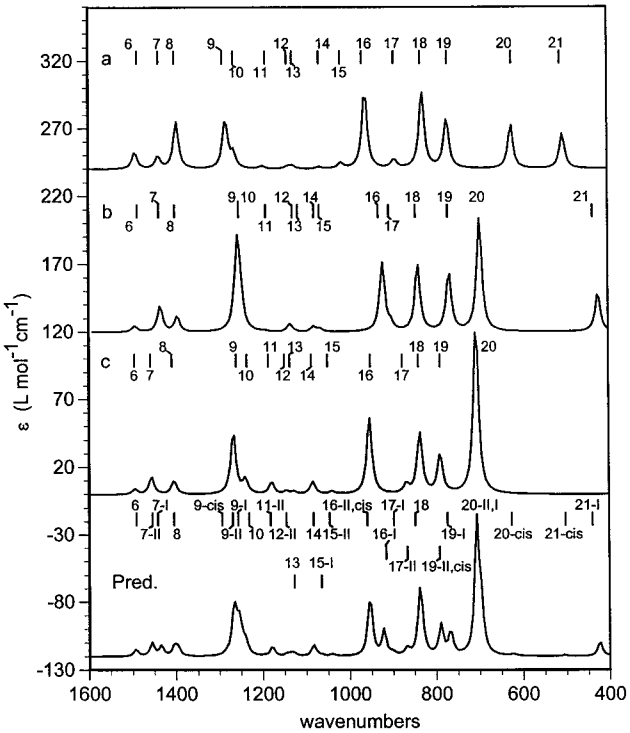

Figure 4. Ab initio vibrational absorption spectra for three conformers of (*S*)-epichlorohydin obtained with the B3LYP/6-311G(2d, 2p) basis set. The spectra were simulated with Lorentzian band shapes and 8-cm^{-1} half-widths and frequencies were multiplied by 0.975. The labels on the traces are the conformation labels (Figure 1). The predicted spectrum (bottom trace) is obtained by adding the population-weighted absorption spectra of all conformers (gauche II, 65.3%; gauche I, 31.6%). The labels for the peaks are same as those in Table 6.

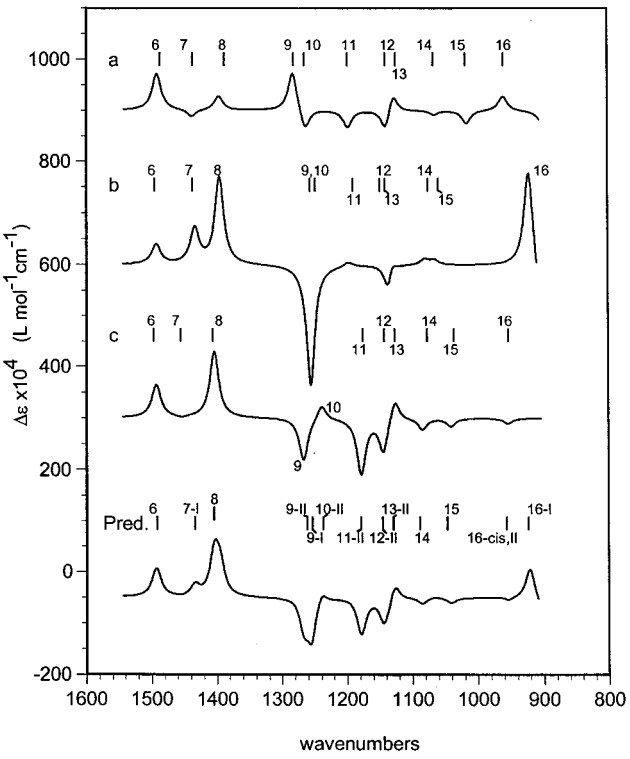

Figure 5. Ab initio VCD spectra for three conformers of (*S*)-epichlorohydrin obtained with the B3LYP/6-311G(2d, 2p) basis set. The spectra were simulated with Lorentzian band shapes and 8-cm^{-1} half-widths, and frequencies were multiplied by 0.975. The labels on the traces are the conformation labels (Figure 1). The predicted spectrum (bottom trace) is obtained by adding the population-weighted VCD spectra of all conformers (gauche II, 65.3%; gauche I, 31.6%). The labels for the peaks are same as those in Table 6.

intensity of ν_{16-I} is far greater than that of $\nu_{16-II,cis}$ (intensity of the latter is essentially zero). This relative intensity pattern for ν_{16} is present in the VCD spectra of CCl_4 and CS_2 solutions as well and is reproduced in the calculated spectra with corresponding compositions. The VCD intensity of ν_{7-I} is greater than that of ν_6 in the neat liquid spectrum and the opposite is true in CCl_4 solution spectrum. Although the Cal.3 spectrum correctly reproduces this pattern seen in CCl_4 solution, the Cal.1 spectrum does not reproduce well the pattern seen in neat liquid VCD spectrum. Although some differences still exist, the predicted spectra, obtained with appropriate compositions for neat liquid and inert organic solvents, are close to the respective experimental spectra.

Thus, based on the absorption and VCD spectra, it appears that in the neat liquid-phase, the population of the gauche-I (more polar) is greater than that of the gauche-II conformation, and the opposite is true in nonpolar organic solvents CCl_4 and CS_2. In both cases, the population of the cis conformer is very small. This conclusion is not in agreement with that of Lee et al.,[2d] who suggested that the gauche-I conformer is the most stable form and that the cis conformer is the second most stable one in liquid samples. We can rule out their suggestion of the cis conformer being the second most dominant form unequivocally for the following reason: The ab initio predicted frequencies (Table 6) for ν_9 are 1267, 1256, and 1282 cm^{-1}, respectively, for the gauche II, gauche I, and cis conformers. For this band, the gauche II and gauche I conformers have negative VCD intensities, whereas the cis conformer has positive VCD intensity. Because the frequency of ν_9 for the cis conformer is well separated from those for the gauche II and gauche I conformers, any significant amount of cis conformer will lead to the appearance of positive VCD intensity for ν_{9-cis}. But the experimental VCD spectra do not show any indication of positive VCD intensity at the location of ν_{9-cis}. Simulated spectra indicate that any amount of the cis form that is greater than 10−15% should be detectable in the experimental VCD spectrum. Because positive VCD intensities are not seen in any of the experimental VCD spectra (Figure 3) around 1280 cm^{-1}, we have to conclude that the population of the cis conformer in neat liquid or in solutions is <10−15%, which is supported by populations deduced from absorption intensities (Table 7).

The solvent influence on the conformer compositions can be explained from the populations obtained in different solvents (Table 7). As the dipole moment of the solvent increases, the population of the gauche I conformer increases and that of the gauche II decreases. The dipole moments of the gauche I, gauche II, and cis conformers obtained in the B3LYP/6-311G(2d, 2p) calculation are, respectively, 11.05×10^{-30}, 2.280×10^{-30}, and 9.075×10^{-30} C·m. Because these results follow the order gauche I > cis > gauche II, it can be expected that dipole−dipole interactions are maximum for the gauche I conformer and minimum for the gauche II conformer; hence, the gauche I conformer would be favored over the gauche II conformer in polar media. The same reasoning would explain the sole presence of the gauche I conformer in the solid state. The dipole−dipole interactions with the cis conformer presumably would not sufficiently compensate for the intrinsically unfavorable internal energy of the cis conformer (see Table 1). As a result, the population of the cis conformer remained essentially the same in different solvents. Because both of the inert solvents CCl_4 and CS_2 have no dipole moment, one might at first sight expect no differences in populations in these solvents. But the refractive index (and hence polarizability) of CS_2 is

TABLE 7: Solvent Influence on the Composition of Epichlorohydrin

solvent	dipole moment μ[a] (10^{-30} C m)	relative intensity[b] 16-II, cis/16-I	relative intensity[b] 21-cis/21-I	population (%) g II	population (%) g I	population (%) cis
neat liquid	6.74	0.9464	0.1638	35.7	54.6	9.7
CH_2Cl_2	5.24	0.9957	0.1646	37.2	53.3	9.5
CH_3I	4.50	1.2093	-	42.2	48.5	9.3[c]
$CHCl_3$	3.37	1.3975	0.1881	46.1	44.8	9.1
CS_2	0	1.6595	0.1904	51.0	40.6	8.4
CCl_4	0	2.1993	0.2024	58.6	34.0	7.4
Isolated molecule[d]	-	-	-	65.3	31.6	3.1

[a] Dipole moments for the solvents are from ref 12; listed dipole moment for neat liquid is the experimental dipole moment of epichlorohydrin in cyclohexane from ref 6. [b] Experimental band intensities were obtained by integrating the band areas using BGRAMS software. [c] The intensity of 518 cm^{-1} band could not be determined because of solvent interference. Thus, the cis population was assumed based on the calculated cis populations of epichlorohydrin in other solvents. [d] From B3LYP/6-311G(2d,2p) calculation of Gibbs energies.

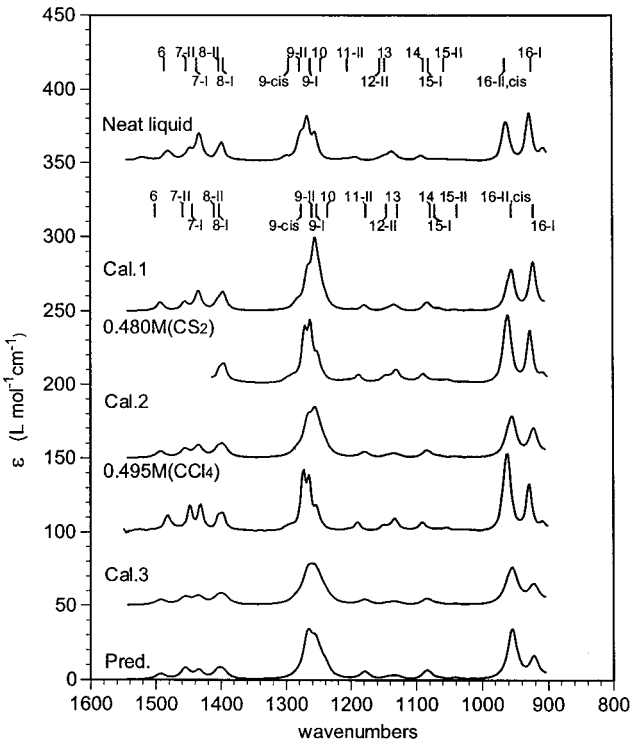

Figure 6. Comparison of the experimental absorption spectra (in neat liquid, CS_2 solution, and CCl_4 solution) of (+)-epichlorohydrin with the predicted absorption spectra. The predicted spectra were simulated with Lorentzian band shapes and 8-cm^{-1} half-widths, and ab initio frequencies were multiplied by 0.975. The labels on the experimental traces give concentration and solvent employed for the experimental spectra. The labels for predicted spectra are as follows. Cal.1: 35.7% gauche II, 54.6% gauche I, and 9.7% cis; Cal.2: 51% gauche II, 40.6% gauche I, and 8.4% cis; Cal.3: 58.6% gauche II, 34.0% gauche I, and 7.4% cis; Pred.: 65.3% gauche II, 31.6% gauche I, and 3.1% cis.

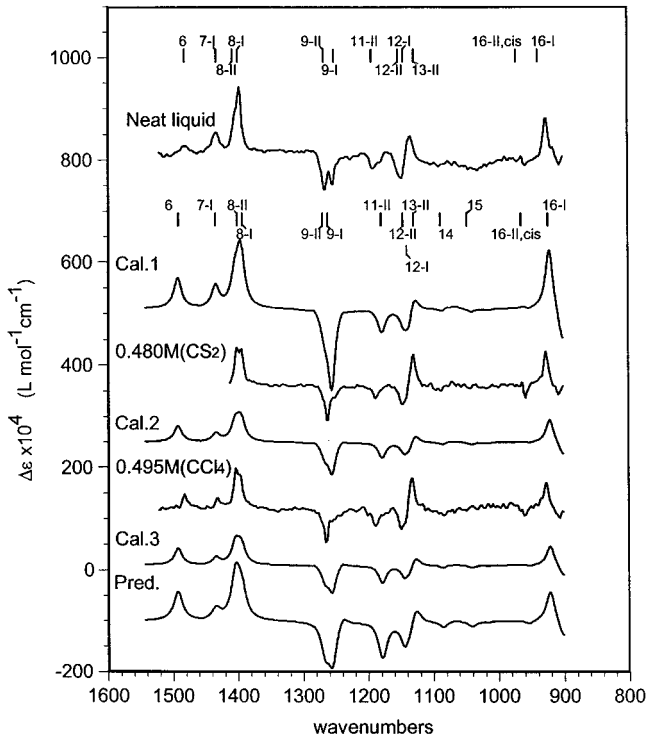

Figure 7. Comparison of the experimental VCD spectra (in neat liquid, CS_2 solution, and CCl_4 solution) of (+)-epichlorohydrin with the predicted VCD spectra for (S)-epichlorohydrin. The predicted spectra were simulated with Lorentzian band shapes and 8-cm^{-1} half-widths, and ab initio frequencies were multiplied by 0.975. The labels on the experimental traces give concentration and solvent employed for the experimental spectra. The labels for predicted spectra are as follows. Cal.1: 35.7% gauche II, 54.6% gauche I, and 9.7% cis; Cal.2: 51% gauche II, 40.6% gauche I, and 8.4% cis; Cal.3: 58.6% gauche II, 34.0% gauche I, and 7.4% cis; Pred.: 65.3% gauche II, 31.6% gauche I, and 3.1% cis.

larger[12] than that of CCl_4, so the dipole−induced dipole interactions can be expected to be larger in CS_2 than in CCl_4. The populations given in Table 7 appear to support this view.

Summary

The comparison of experimental and ab initio predicted absorption and VCD spectra indicates that (*S*)−(+)-epichlorohydrin in various liquid solutions exists predominantly in the gauche I and gauche II conformations and the amount of cis conformation is <10%. The population of the gauche I conformer is larger than that of the gauche II conformer in neat liquid and the opposite is true in nonpolar solvents. In other organic solvents, the population of the gauche I conformer increases with increasing dipole moment of the solvent.

Acknowledgment. Grants from NSF(CHE9707773) and Vanderbilt University are gratefully acknowledged.

References and Notes

(1) (a) Kawamura, K.; Ohta, T.; Otani, G., *Chem. Pharm. Bull.* **1990**, *38*, 2092. (b) *Tetrahedron: Asymmetry* **1993**, 4, 961, 2265.

(2) (a) Hayashi, M.; Hamo, K.; Ohno, K.; Murata, H. *Bull. Chem. Soc. Jpn.* **1972**, *45*, 949. (b) Charles, S. W.; Jones, G. I. L.; Owen, N. L. *J. Mol. Struct.* **1974**, 20, 83. (c) Kalasinsky, V. F.; Wurrey, C. J. *J. Raman Spectrosc.* **1980**, 9, 315. (d) Lee, M. J.; Hur, S. W.; Durig, J. R. *J. Mol. Struct.* **1998**, 444, 99.

(3) (a) Thomas, W. A. *J. Chem. Soc. B.* **1968**, 1187. (b) MacDonald, C. J.; Reynolds, W. F. *Can. J. Chem.* **1970**, *48*, 1046. (c) Shapiro, M. J. *J. Org. Chem.* **1977**, 42, 1434.

(4) (a) Fujiwara, F. J.; Chang, J. C.; Kim, H., *J. Mol. Struct.* **1977**, 41, 177. (b) Fujiwara, F. J.; Painter, J. L.; Kim, H. *J. Mol. Struct.* **1977**, 41,

169. (c) Mohammadi, M. A.; Brooks, W. V. F. *J. Mol. Spectrosc*. **1978**, *73*, 353. (d) Mohammadi, M. A.; Brooks, W. V. F. *J. Mol. Spectrosc*. **1979**, 78, 89.

(5) Shen, Q. *J. Mol. Struct*. **1985**, *130*, 275.

(6) Aroney, M. J.; Calderbank, K. E.; Stootman, H. J. *Aust. J. Chem*. **1978**, *31*, 2303.

(7) (a) Ashvar, C. S.; Devlin, F. J.; Stephens, P. J. *J. Am. Chem. Soc.* **1999**, *121*, 2836. (b) Gigante, D. M. P.; Long, F.; Bodack, L. A.; Evans, J. M.; Kallmerten, J.; Nafie, L. A.; Freedman, T. B. *J. Phys. Chem.* **1999**, *103*, 1523. (c) Tam, C. N.; Bour, P.; Keiderling, T. A. *J. Am. Chem. Soc.* **1996**, *118*, 10285. (d) Diem, M. *Introduction to Modern Vibrational Spectroscopy*; John Wiley & Sons: New York, 1994; (e) McCann, J. L.; Rauk, A.; Wieser, H. *Can. J. Chem*. **1998**, 76, 274. (f). Polavarapu, P. L.; Zhao, C.; Cholli, A.; Vernice, G. *J. Phys. Chem B.* **1999**, *103*, 6127.

(8) *Gaussian 98, Revision A.3*, Frisch, M. J.; Trucks, G. W.; Schlegel, H. B.; Scuseria, G. E.; Robb, M. A.; Cheeseman, J. R.; Zakrzewski, V. G.; Montgomery, Jr., J. A.; Stratmann, R. E.; Burant, J. C.; Dapprich, S.; Millam, J. M.; Daniels, A. D.; Kudin, K. N.; Strain, M. C.; Farkas, O.; Tomasi, J.; Barone, V.; Cossi, M.; Cammi, R.; Mennucci, B.; Pomelli, C.; Adamo, C.; Clifford, S.; Ochterski, J.; Petersson, G. A.; Ayala, P. Y.; Cui, Q.; Morokuma, K.; Malick, D. K.; Rabuck, A. D.; Raghavachari, K.; Foresman, J. B.; Cioslowski, J.; Ortiz, J. V.; Stefanov, B. B.; Liu, G.; Liashenko, A.; Piskorz, P.; Komaromi, I.; Gomperts, R.; Martin, R. L.; Fox, D. J.; Keith, T.; Al-Laham, M. A.; Peng, C. Y.; Nanayakkara, A.; Gonzalez, C.; Challacombe, M.; Gill, P. M. W.; Johnson, B.; Chen, W.; Wong, M. W.; Andres, J. L.; Gonzalez, C.; Head-Gordon, M.; Replogle, E. S.; Pople, J. A., Gaussian, Inc.: Pittsburgh, PA, 1998.

(9) Becke, A. D. *J. Chem. Phys*. **1993**, *98*, 1372, 5648.

(10) Cheeseman, J. R.; Frisch, M. J.; Devlin, F. J.; Stephens, P. J. *Chem. Phys. Lett*. **1996**, 252, 211.

(11) Schachtschneider, J. H. *Vibrational analysis of polyatomic molecules*, Reports 231/64 and 57/65, Shell Development Company, Houston, TX, 1962.

(12) Atkins, P. W. *Physical Chemistry*, 5th ed.; Oxford University Press: New York, 1994; Alberty, R. *Physical Chemistry*, 6th ed.; John Wiley & Sons: New York, 1983.